

Detection of weak and overlapping pulses from waveform airborne laser scanning data

Yu-Ching Lin¹, Jon Mills² & Sarah Smith-Voysey³

¹ Geomatic Engineering, Newcastle University, UK; yu-ching.lin@ncl.ac.uk

² Geomatic Engineering, Newcastle University, UK; j.p.mills@ncl.ac.uk

³ Research, Ordnance Survey, UK; Sarah.Smith-Voysey@ordnancesurvey.co.uk

Abstract

Airborne laser scanning has become a popular technique to estimate canopy height and forest structure. However, current discrete laser scanning systems still suffer the limitation of 3m multi-target resolution and the loss of information about range estimation. In order to improve range resolution and accuracy, new generation small-footprint waveform laser scanning data were investigated. A new approach was developed to detect targets from complex overlapping and weak pulses, which are likely to occur in vegetated areas. The algorithm is based on the popular Gaussian decomposition method and contains two main processing procedures. The shapes of overlapping pulses are analysed to find visible peaks and overlapping peaks, and then reasonable constraints and checks are applied to the fitting process. The test results showed the developed detection algorithm resolved overlapping pulses very well as long as the pulse shapes illustrated asymmetric behaviour or a non-Gaussian distribution. Weak pulses exhibiting a Gaussian shape were also successfully detected.

Keywords: laser scanning, waveform, detection

1. Introduction

Airborne laser scanning has developed rapidly to become the technique of choice for high resolution terrain model generation and detailed vertical distribution of canopy structure in vegetated areas. Current pulsed laser scanning systems are based on time-of-flight techniques to estimate range distances between scanners and targets. Pulse detection methods are applied to detect targets and determine range in order to measure the elapsed time. However, different methods can result in different range resolution (i.e. the ability to differentiate two neighbouring targets from one another) and different range accuracy (i.e. the ability to seek the corresponding positions from transmitted and received pulses) (Baltsavias, 1999; Wagner et al., 2004b; Jutzi and Stilla, 2005). Inaccurate range determination obviously reduces the accuracy of the three-dimensional laser points (Baltsavias, 1999), thereby indirectly affecting the estimate of forest characteristics (e.g. canopy height). In order to meet the demand for high accuracy applications, studies into range estimation are therefore necessary.

In general, typical pulse detection methods applied in discrete laser scanning systems are normally threshold-based (e.g. peak detection, leading edge detection, constant fraction detection) - (Lemmens, 2007). Return pulses with strong, nearly perfect peaks are primarily detected. The common difficulty, however, is to detect weak pulses and complex overlapping pulses, which are likely to occur in vegetated areas. Weak pulses below the threshold go undetected and information about targets which present low reflectance or have been observed at a distance is discarded (e.g. ground information under canopy). On the other hand, when the distance between successive targets diminishes, overlapping pulses are present (Baltsavias, 1999; Wiechert, 2004). The shapes of overlapping pulses are variable and can differ significantly to standard returns, making it virtually impossible for typical pulse detection methods to resolve targets correctly. Therefore, multi-target resolution is seriously limited

(Baltsavias, 1999; Katzenbeisser, 2003) and range distance can be inaccurately estimated (Jutzi and Stilla, 2006). For example, when overlapping pulses occur in areas of low vegetation, ground height could be overestimated. Wiechert (2004) has emphasised that the capability of target separation has a great impact on the quality of elevation models derived from laser scanning data.

Established discrete laser scanning systems only provide three-dimensional coordinates of points and their associated intensity values. Users are unable to determine the errors caused due to the limitations of the pulse detection methods used because the information about range estimation is missing. Moreover, most systems only capture first and (or) last return, or up to four returns, the information in between have been discarded. Commercial small-footprint waveform airborne laser scanning systems have recently become available that store the entire waveform of each received pulse, thereby offering users the opportunity to apply their own pulse detection methods in order to detect targets and define ranges. This creates significant opportunities to overcome the shortcomings of typical pulse detection methods. New potential for improving the classification of laser points is also expected using waveform data (Flood, 2001; Pfeifer et al., 2004; Wagner et al., 2004a) since the characteristics of targets are believed to be present in the waveform (Brenner et al., 2003).

Since 2004, new generation commercial small-footprint waveform laser scanning systems have emerged on the market (Hug et al., 2004; Lemmens, 2007) and there has been an increasing interest in maximising the potential of waveform data. Wagner et al. (2007) investigated the emerging benefits of using this new waveform data. In general, studies have focussed on overcoming the limitation of discrete laser scanning systems. For example, various detectors have been developed to extract more laser points than discrete systems (Persson et al., 2005; Nordin, 2006; Reitberger et al., 2006). However, little attention has been paid to detecting targets from complex pulses and validating results. On the other hand, parameters related to target characteristics have been extracted from waveform data in order to improve the classification of laser points, which has been a popular and challenging research issue for discrete data (Doneus and Briese, 2006; Wagner et al., 2006; Mandlburger et al., 2007). Thus far, the relationship between target characteristics and derived parameters has not been studied in detail and not widely examined over different land cover types (Doneus and Briese, 2006; Mandlburger et al., 2007; Pfeifer and Briese, 2007). More research effort is required into the issue of whether this so-called additional information can offer more reliable analysis for different applications and how to integrate it with other datasets (Jutzi and Stilla, 2005; Mandlburger et al., 2007; Pfeifer and Briese, 2007).

This paper presents a method to detect targets from weak and overlapping pulses in order to achieve high range resolution and accuracy. The method also provides an important foundation for extracting the correct surface features of individual targets. The overview of waveform data derived from a Riegl LMS-Q560 is introduced in Section Two. Section Three presents the details of the developed method. Section Four contains a qualitative validation and comparison with commercial software. Finally, the main findings of the study are summarised in Section Five.

2. Full-waveform data

Waveform data from a Riegl LMS-Q560 full-waveform laser scanner were used in this study. The specifications of this laser scanner are presented in Ullrich et al. (2008). For each timestamp the transmitted waveform, received waveform and scan angle are stored. The sampling rate for digitising the waveform is 1GHz. The waveform is constructed as an amplitude-against-time dataset. The shape of transmitted waveforms is a Gaussian-like distribution (Wagner et al., 2006) as shown in Figure 1 (a). The received waveform is the record

of the returned energy from each laser pulse and can vary with the height distribution of the illuminated surface (Harding et al., 1994). The simplest cases of received waveforms are composed of nearly perfect peaks. For example, Figure 1 (b) shows the received waveform with two returns which are both similar to the shape of the transmitted pulse. More difficult cases are waveforms with complex shapes which are not like the transmitted pulse (see Figure 2). Moreover, waveforms with weak pulses also exist (see Figure 1(c)).

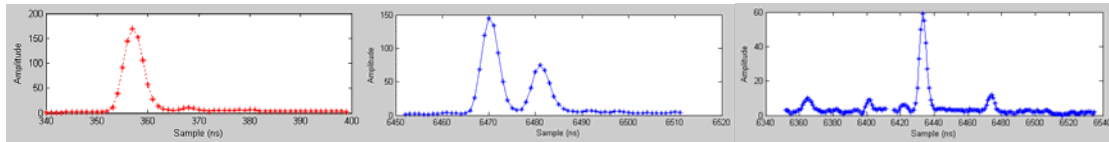


Figure 1: (a) Example of transmitted waveform (b) Received waveform with nearly perfect peaks (c) Received waveform with weak pulses (note Y-axis scale change for illustrative purposes)

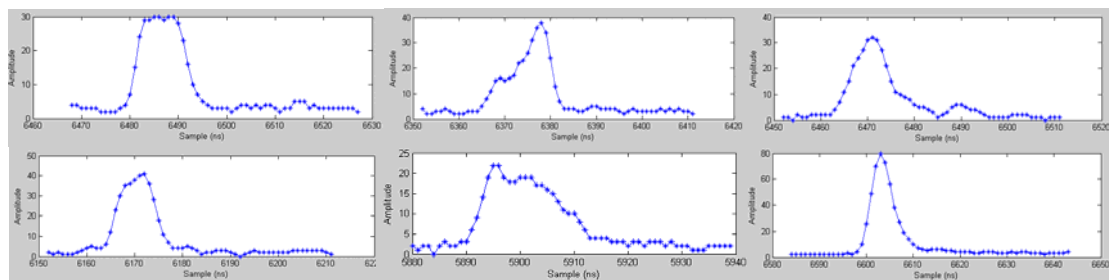


Figure 2: Received waveforms with complex shapes (note Y-axis scale change for illustrative purposes)

After examining different examples of typical received waveforms, a number of questions stand out:

- How many individual targets are hidden within a complex waveform?
- Where is the relative point for range estimation?
- Are weak pulses targets or noise?

A method was developed to seek the answers for the above questions and is described in Section Three.

3. Methodology

Because pulses are transmitted with a Gaussian-like distribution, the Gaussian decomposition method can be used for range estimation. This assumes that each return is Gaussian in nature and that the received signal is a sum of individual Gaussian distributions (Hofon et al., 2000). Fitting Gaussian functions to waveform data provides each return with a parametric description which can be used to store pulse shape information and decreases the effect of noise. Hofon et al. (2000) and Jutzi and Stilla (2005) concluded that the Gaussian decomposition method can improve the accuracy of range measurement compared with algorithms using only single values (e.g. peak algorithm, leading edge algorithm). The algorithm developed herein is therefore based on the Gaussian decomposition method. Waveform data from each laser pulse can be modelled using equation (1). The width parameter is $\sqrt{2}$ times the standard deviation of the Gaussian peak.

$$y = N_{level} + \sum_{i=1}^n A_i \exp \left[- \left(\frac{t - t_i}{width_i} \right)^2 \right] \quad (1)$$

Where A = the amplitude of i th Gaussian t_i = the i th Gaussian peak

N_{level} = noise level of the waveform n = the number of Gaussians
 $width_i$ = pulse width of i th Gaussian

In order to get good fits and reasonable estimates, two main processing procedures are applied.

3.1 Initial Parameter Estimates

Reasonable initial estimates of the number of targets to be detected and the coefficients of Gaussian functions are needed for good fits to be achieved. The main task of this procedure is finding potential peak positions from weak and overlapping pulses. Firstly, visible peaks need to be found for the presence of standard returns. Figure 3 shows the workflow adopted for finding visible peaks. Local maxima are selected as the candidates for visible peaks. A_T is a threshold to separate signal from background noise. A more stringent check is further applied on weak visible peaks (A_S is the threshold for selecting weak peaks) and neighbouring samples since only weak returns with pulse-like shapes should be identified as illuminated targets. In addition, the separation between two visible peaks must be greater than half the pulse length. Any peaks found within this distance are treated as noise. This is based on the assumption that when the separation between two Gaussian components diminishes to less than one pulse length, there is only one main peak existing, and at separations of less than half a pulse length, pulses become entirely like one standard Gaussian distribution. This assumption is demonstrated using simulated data and illustrated in Figure 4.

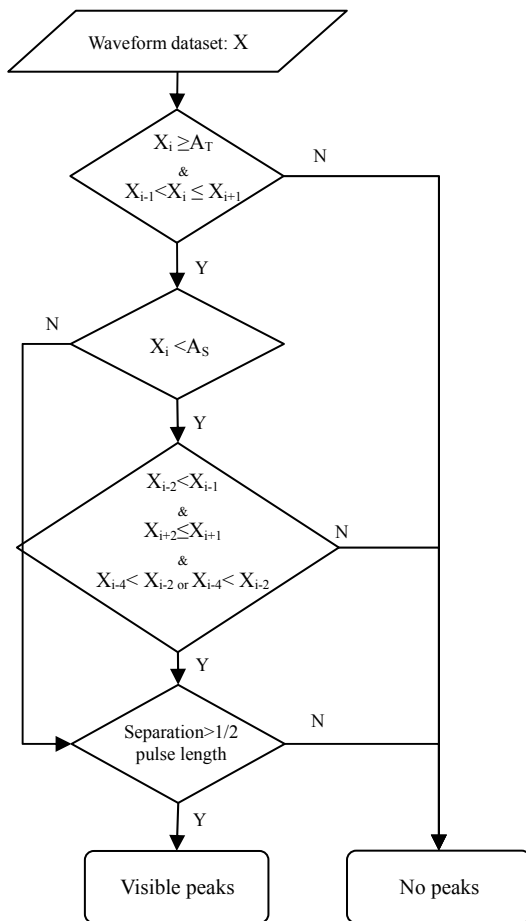


Figure 3: Flowchart for finding visible peaks

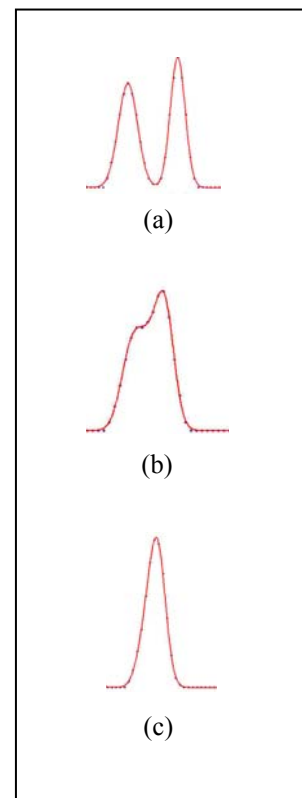


Figure 4: Simulation of received waveform from two returns with different separation (a): 3 pulse length (b): 1 pulse length (c): 1/2 pulse length

Based on the above assumptions, in order to resolve overlapping pulses, the shapes of pulses are analysed to find overlapping peaks. The flowchart for this stage is presented in Figure 5. Essentially, the algorithm looks for asymmetric pulses. It is implemented to find inflexion points on both sides of primary visible peaks. In addition, in order to decrease the sensitivity of finding inflexion points caused by noise effects, step (a) in Figure is applied. Step (b) limits the place where overlapping peaks can be identified to avoid detecting spurious peaks from background noise. Finally, if the number of samples on the edge of a primary peak is much greater than those on the edge of the transmitted pulse, one overlapping peak is forced to exist. Figure 6 shows the examples of detecting visible and overlapping peaks. Once visible and overlapping peaks are detected, initial values for the corresponding amplitude and timing point will also be selected. An initial width value for each Gaussian component is chosen to be the same value as the width of the transmitted pulse.

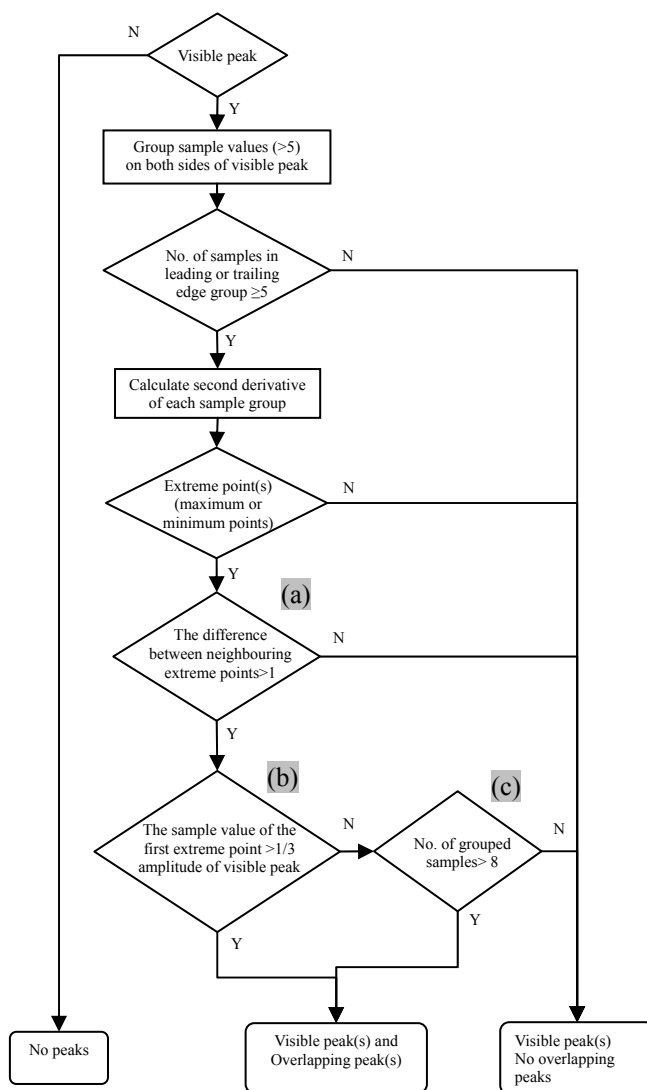


Figure5: Flowchart for finding overlapping peaks

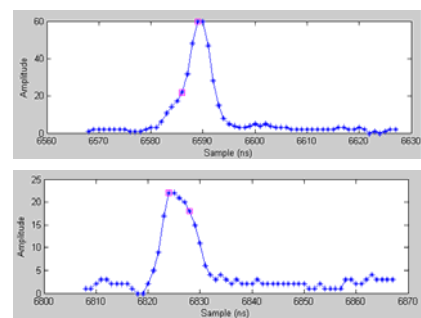


Figure 6: Examples of detecting visible and overlapping peaks

3.2 Parameter Optimization

In order to identify any peaks missed during the first procedure, remove noise, and determine the best estimation of peak positions, Gaussian fitting with reasonable constraints and checks are applied. The flowchart for this stage is presented in Figure 7. In the fitting process, a non-linear optimization technique – the Trust Region algorithm (Branch et al., 1999) – is used to apply constraints on parameter estimates. The lower boundary for Gaussian amplitude is specified as 2, which is the DC offset value, to avoid erroneous estimation. At first, initial parameter estimates from the first procedure (refer to Section 3.1) are used in Gaussian-fitting. Residual maximums from the Gaussian fit are checked to find the peaks missed during the first procedure. Since the ringing effect generates spurious small peaks immediately after pulses with high amplitudes, in order to avoid finding the peaks resulting from ringing, the corresponding amplitude of the sample with high residual value is further checked. Step (a) in Figure 7 selects ambiguous peaks which could result in overlapping and weak pulses to perform further checks, otherwise individual Gaussian parameters are taken as the best estimation. Step (b) contains final checks for reasonable parameter estimates. If any unreasonable parameter is found, the peak will be removed. The constraints are applied on special cases. Sep < 2ns is to limit the minimum separation between two peaks to 2ns, which is 1/2 pulse length of the Riegl LMS-Q560 system, based on the assumption described in Section 3.1. In order to avoid erroneous estimates, thresholds for estimated amplitude and width are applied (e.g. $A < A_{min}$, $Width > \sigma_{max}$, $Width < \sigma_{min}$). Moreover, $A < (Max(x))/10$ & $D_{is} < S_r$ & $Max(x) > P_m$ is set to remove peaks generated by the ringing effect. To prevent detecting background noise, $A < A_w$ & ($Width > \sigma_{wi}$ or $< \sigma_{wm}$) is set to limit the width boundary of extreme weak pulses and $A < A_d$ & $Width > \sigma_d$ is the constraint for potential weak pulses. Finally, $Sep < S_o$ & $DW < D_o$ is applied to check the width difference between two extremely-overlapping pulses whose separation is close to half the pulse length. It is assumed that the width difference between two overlapping peaks must be big enough to allow the presence of a non-Gaussian shape.

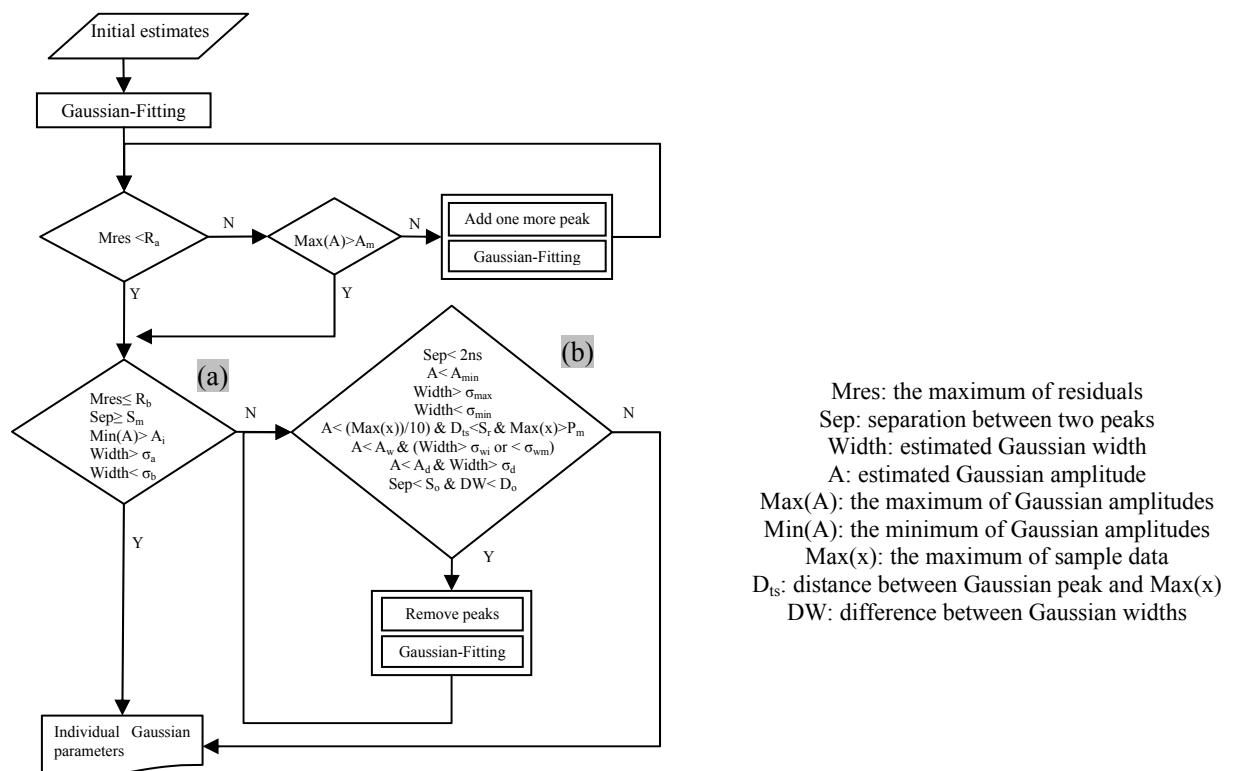


Figure 7: Flowchart for the best estimation of the number of targets and peak positions

4. Results

Waveform data from a Riegl LMS-Q560 full-waveform laser scanner were collected over different land cover classes in Bristol, United Kingdom in August 2006 and used to test the developed approach. Qualitative validation for the detection of overlapping pulses and weak pulses was performed by examining 3D points and orthoimages acquired from the same platform. The performance was compared with commercial software which also processes waveform data.

4.1 Qualitative Validation for Overlapping Pulses

In Great Britain the height of most safety barriers along motorways is 0.61 ± 0.03 m from the ground to the centre of the barrier beams (Wignall et al., 1999). This height can result in overlapping pulses if lasers hit both the barrier and the ground within the footprint. In order to validate the result of resolving overlapping pulses, waveforms that interacted with vehicle safety fences were investigated. Figure 8 shows a sample of examined motorway and red points represent laser points known to interact with safety barriers. Figure 9 (a) and (b) shows sections of laser points as derived from commercial software and the developed algorithm respectively. Figure 9(c) illustrates the corresponding waveforms. It is apparent that the developed algorithm resolved overlapping pulses very well, and the hidden peaks were successfully found. It is evident that more points were extracted using the developed algorithm than with the commercial software.



Figure 8: Examined motorway in Bristol

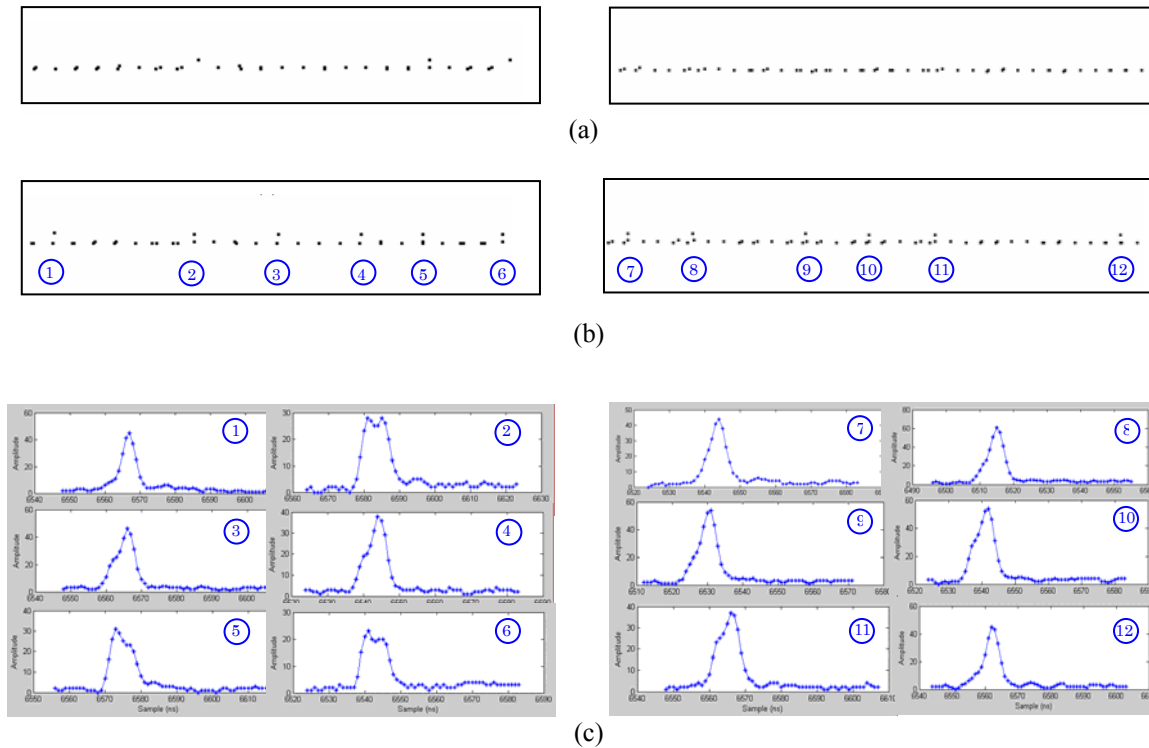


Figure 9: (a) Points from commercial software (b) points from the developed algorithm (c) corresponding waveforms

4.2 Qualitative Validation for Weak Pulses

Figure 10 shows an example of detecting weak pulses in a vegetated area. Red points represent 3D points with low amplitude. Compared with the commercial software, weak pulses are more likely to be detected using the developed algorithm. Interestingly, numerous weak pulses occurred at positions of potential ground points beneath forest canopies. This implies that these laser pulses penetrated the vegetation to the ground level, but the energy of the last returns was very weak to the point of being undetectable by the commercial algorithm.

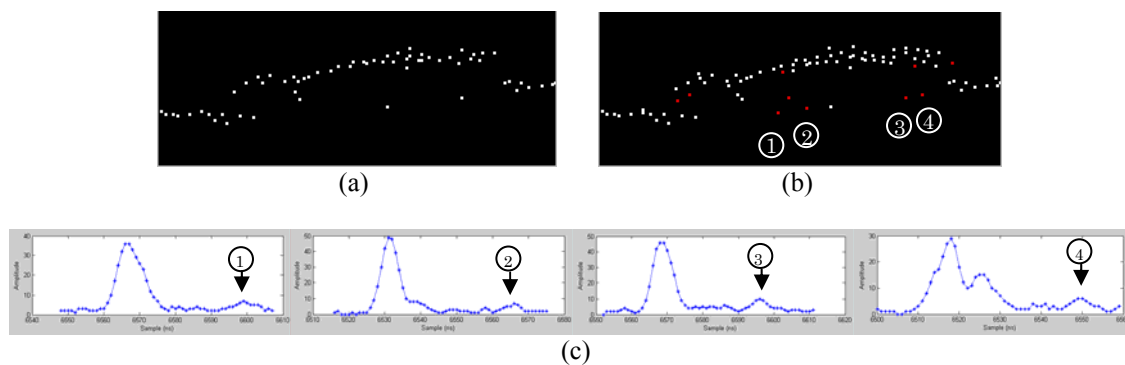


Figure 10: (a) Points from commercial software (b) points from developed algorithm (c) corresponding waveforms

5. Conclusion

This paper has presented a new approach to resolve overlapping pulses and detect weak pulses from small-footprint waveform laser scanning data. The results show the shapes of overlapping pulses were found to be variable and depend on the amplitude, widths and separation distance of overlaid individual pulses. Due to the success of finding overlapping peaks, multi-target resolution has been improved. Moreover, the range accuracy will be improved as peak positions from individual returns are successfully identified. This benefit can potentially reduce the risk of overestimating ground height in vegetated areas. On the other hand, successfully detecting weak pulses can offer the opportunity to acquire more accurate digital terrain models in vegetated areas. Further research is being performed to provide a quantitative validation of these findings, as well as exploring the benefits of waveform parameters (amplitude, width and range) which are extracted after successfully identifying individual targets. It is expected that these waveform parameters offer additional information to further discriminate between on- and off-terrain points, thereby further enhancing outputs from airborne laser scanning.

References

- Baltsavias, E.P., 1999. Airborne laser scanning: basic relations and formulas. *ISPRS Journal of Photogrammetry & Remote Sensing*, 54: 199-214.
- Branch, M.A., Coleman, T.F. and Li, Y., 1999. A Subspace, Interior, and Conjugate Gradient Method for Large-Scale Bound-Constrained Minimization Problems. *SIAM Journal on Scientific Computing*, 21(1): 1-23.
- Brenner, A.C., Zwally, H.J., Bentley, C.R., Csatho, B.M., Harding, D.J., Hofton, M.A., Minster, J.-B., Roberts, L., Saba, J.L., Thomas, R.H. and Yi, D., 2003. Geoscience Laser Altimeter System (GLAS) - Derivation of Range and Range Distributions From Laser Pulse Waveform Analysis for Surface Elevations, Roughness, Slope, and Vegetation Heights. <http://www.csr.utexas.edu/glas/atbd.html> [Accessed: December 2006].
- Doneus, M. and Briese, C., 2006. Digital terrain modelling for archaeological interpretation within forested areas using full-waveform laserscanning. *The 7th International Symposium on Virtual Reality, Archaeology and Cultural Heritage VAST*, Athens, Greece. 155-162.
- Flood, M., 2001. Lidar activities and research priorities in the commercial sector. *International Archives of Photogrammetry and Remote Sensing*, 34(3/W4): 3-7.
- Harding, D.J., Blair, J.B., Garvin, J.B. and Lawrence, W.T., 1994. Laser altimetry waveform measurement of vegetation canopy structure. *Geoscience and Remote Sensing Symposium, 1994. IGARSS '94. Surface and Atmospheric Remote Sensing: Technologies, Data Analysis and Interpretation., International*. 1251-1253
- Hofton, M.A., Minster, J.B. and Blair, J.B., 2000. Decomposition of Laser Altimeter Waveforms. *IEEE Transactions on Geoscience and Remote Sensing*, 38(4): 1989-1996.
- Hug, C., Ullrich, A. and Grimm, A., 2004. Litemapper-5600 – A waveform-digitizing LIDAR terrain and vegetation mapping system. *International Archives of Photogrammetry, Remote Sensing and Spatial Information Sciences*, 36(8/W2): 24-29.
- Jutzi, B. and Stilla, U., 2005. Measuring and processing the waveform of laser pulses. *Optical 3-D Measurement Techniques VII*, 1: 194-203.
- Jutzi, B. and Stilla, U., 2006. Range determination with waveform recording laser systems using a Wiener Filter. *ISPRS Journal of Photogrammetry & Remote Sensing*, 61(2): 95-107.
- Katzenbeisser, R., 2003. *Technical note on: Echo detection*, TopoSys GmbH, Germany.
- Lemmens, M., 2007. *Product Survey on Airborne Lidar Sensors*, GIM International, 21 (2)
- Mandlburger, G., Briese, C. and Pfeifer, N., 2007. Progress in LiDAR sensor technology - chance and challenge for DTM generation and data administration. *Photogrammetric Week 2007*. 159-169.

- Nordin, L., 2006. *Analysis of waveform data from airborne laser scanner systems*. Master Thesis, Lulea University of Technology.
- Persson, Å., Söderman, U., Töpel, J. and Ahlberg, S., 2005. Visualization and analysis of full-waveform airborne laser scanner data. *International Archives of Photogrammetry, Remote Sensing and Spatial Information Sciences*, 36(3/W19): 103-108.
- Pfeifer, N. and Briese, C., 2007. Geometrical aspects of airborne laser scanning and terrestrial laser scanning. *International Archives of Photogrammetry and Remote Sensing*, 36(3/W52): 311-319.
- Pfeifer, N., Gorte, B. and Elberink, S.O., 2004. Influences of vegetation on laser altimetry - analysis and correction approaches. *International Archives of Photogrammetry, Remote Sensing and Spatial Information Sciences*, 36(8/W2): 283-287.
- Reitberger, J., Krzystek, P. and Heurich, M., 2006. Full-waveform analysis of small footprint airborne laser scanning data in the Bavarian forest national park for tree species classification. *Workshop on 3D Remote Sensing in Forestry*: 218-227.
- Ullrich, A., Studnicka, N., Hollaus, M., Briese, C., Wagner, W., Doneus, M. and Mücke, M., 2008. Improvements in DTM generation by using full-waveform airborne laser scanning data.
http://www.riegl.com/airborne_scanners/airborne_photo_gallery/downloads/Ullrich_et_al_2007_Moskau_engl.pdf [Accessed: 28 Feb, 2008].
- Wagner, W., Eberhöfer, C., Hollaus, M. and Summer, G., 2004a. Robust filtering of airborne laser scanner data for vegetation analysis. *International Archives of Photogrammetry, Remote Sensing and Spatial Information Sciences*, Freiburg, Germany. 56-61.
- Wagner, W., Roncat, A., Melzer, T. and Ullrich, A., 2007. Waveform analysis techniques in airborne laser scanning. *international Archives of Photogrammetry and Remote Sensing*, 36(3/W52): 413-418.
- Wagner, W., Ullrich, A., Ducic, V., Melzer, T. and Studnicka, N., 2006. Gaussian decomposition and calibration of a novel small-footprint full-waveform digitising airborne laser scanner. *ISPRS Journal of Photogrammetry & Remote Sensing*, 60: 100-112.
- Wagner, W., Ullrich, A., Melzer, T., Briese, C. and Kraus, K., 2004b. From single-pulse to full-waveform airborne laser scanners: potential and practical challenge. *International Archives of Photogrammetry, Remote Sensing and Spatial Information Sciences*, 35(B3): 201-206.
- Wiechert, A., 2004. *Linking laser scanning to surveying and visualization*, Geo Informatics, 7, pp. 48-51.
- Wignall, A., Kendrick, P.S., Ancill, R. and Copson, M., 1999. *Roadwork: theory and practice*, 4 Butterworth Heinemann, Zoxford; Boston